Science of the Total Environment 592 (2017) 627–638

Contents lists available at ScienceDirect

Science of the Total Environment

journal homepage: www.elsevier.com/locate/scitotenv

Cause and predictability for the severe haze pollution in downtown Beijing in November–December 2015

Ziyin Zhang [a,b,*], Daoyi Gong [c], Rui Mao [c], Seong-Joong Kim [d], Jing Xu [b], Xiujuan Zhao [b], Zhiqiang Ma [a]

[a] Environmental Meteorology Forecast Center of Beijing-Tianjin-Hebei, Chinese Meteorological Administration, Beijing 100089, China
[b] Institute of Urban Meteorology, Chinese Meteorological Administration, Beijing 100089, China
[c] State Key Laboratory of Earth Surface Processes and Resource Ecology, Beijing Normal University, Beijing 100875, China
[d] Korea Polar Research Institute, Incheon 406-840, Republic of Korea

HIGHLIGHTS

- Anomalous large-scale circulations led to severe haze in Beijing over Nov.–Dec. 2015.
- Abnormal changes at upper troposphere may be the trigger point for the haze events.
- Kinetic energy index could be used to evaluate the clearance capacity of atmosphere.
- The daily (hourly) $PM_{2.5}$ can be predicted in the maximum leading times of 8 (5) days.

GRAPHICAL ABSTRACT

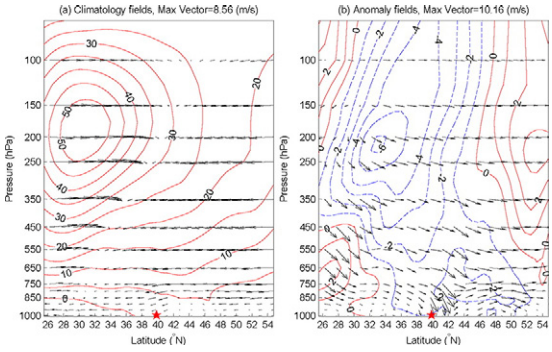

ARTICLE INFO

Article history:
Received 17 December 2016
Received in revised form 31 January 2017
Accepted 2 March 2017
Available online 22 March 2017

Editor: D. Barcelo

Keywords:
Severe haze pollution
$PM_{2.5}$
Meteorological condition
Atmospheric circulation
WRF-Chem

ABSTRACT

Based on the hourly $PM_{2.5}$ concentrations, meteorological variable records and ERA-Interim reanalysis data, a series of diagnostic analyses were conducted to explore the possible meteorological causes for the severe haze pollution that occurred in Beijing in November–December 2015. Using the online-coupled WRF-Chem model and GFS data, the predictability of hourly and daily $PM_{2.5}$ concentrations was evaluated. The results showed that, in the context of pollutant emission, the severe haze pollution in downtown Beijing in November–December 2015 was primarily attributed to anomalous local meteorological conditions, which were caused and strengthened by anomalous large-scale atmospheric circulations. The abnormal changes in the upper troposphere appeared to trigger the anomalies in the middle-lower troposphere and the local conditions. The numerical simulations can capture the spatial distribution patterns of the $PM_{2.5}$ concentrations for predictions of 1 to 10 days in advance. The $PM_{2.5}$ concentration trends in downtown Beijing were generally consistent with the predictions on both daily and hourly time-scales, although the predictability decreased gradually as the lead times prolonged. The predictability of the daily mean $PM_{2.5}$ concentration was slightly higher than that of the hourly concentration. The statistical indices suggested that the predictions of daily and hourly mean $PM_{2.5}$ concentrations were generally skillful and reliable for maximum lead times of 8 and 5 days, respectively.

* Corresponding author.
E-mail address: zzy_ahgeo@163.com (Z. Zhang).

http://dx.doi.org/10.1016/j.scitotenv.2017.03.009
0048-9697/

1. Introduction

Beijing is the capital of China, and it is one of the largest cities in the world, with approximately 20 million residents. With its rapid urbanization and industrial development over the past several decades, Beijing and its adjacent areas are becoming more and more important in China and also for the global economy. However, rapid economic growth and urbanization have increased the level of air pollution in recent decades (Streets et al., 2007; Chan and Yao, 2008; Wang et al., 2010; Gao et al., 2011; Wu et al., 2011; Tie et al., 2015; Zheng et al., 2015b). Beijing and eastern China have frequently suffered from severe haze or smog days in recent years, which were characterized by high particle mass concentrations and low visibility. Severe haze pollution, especially persistent haze days (i.e., in January 2013), have greatly threatened human health and traffic safety. Although most people spend >90% of their time indoors, outdoor air pollutants can penetrate the indoor environment and raise the adverse health effects of pollutant exposure (Ji and Zhao, 2015; Hang et al., 2017). These phenomena have stimulated great interest in studying the haze pollution in Beijing or even eastern China (Wang et al., 2013; Tao et al., 2014; Wang et al., 2014b; Zhang et al., 2014; Wang et al., 2014a; Zhang et al., 2015a; Wang and Chen, 2016; Fu and Chen, 2017; Han et al., 2016). Very serious haze pollution hit Beijing again in November–December 2015, and red alerts were issued for heavy pollution periods on December 7th and 18th, 2015 (in fact, these were not the worst cases over that period according to pollutant concentration records). That was the first time the capital issued a red alert (the most serious level) for air pollution in Chinese history.

Haze pollution is generally attributed to the following two factors: pollutant emissions to the lower atmosphere from fossil fuel combustion, construction and others and unfavorable meteorological diffusion conditions. The air quality or the occurrence of haze pollution is strongly influenced by meteorology. Meteorological factors not only have essential impacts on the accumulation or diffusion, spread and regional transport of air pollutants, but they also have important impacts on the formation of secondary aerosols, which are generated by complicated physical and chemical reactions (Wang et al., 2012; Zhang et al., 2013; Jeong and Park, 2013; Ramsey et al., 2014; Sun et al., 2015; Zheng et al., 2015a; Quan et al., 2015; Marais et al., 2016). In particular, the weather conditions played an essential role in the daily variability of air pollutant concentrations (Whiteaker et al., 2002; Mues et al., 2012; Feng et al., 2014; Wu et al., 2014; Zhang et al., 2015c). Zhang et al. (2016) suggested that there is a close relationship between the winter haze pollution in the Beijing-Tianjin-Hebei region and the atmospheric circulation at middle-high latitudes over a long-term perspective from 1980 to 2015. Other studies have suggested that, on an interannual time-scale, the air pollution across central and eastern China or even South Asia in the winter and summer has a close relationship with East Asian winter and summer monsoons, respectively (Hien et al., 2011; Cao et al., 2015; Cheng et al., 2016; Li et al., 2016).

It was assumed that the emission discharges in Beijing and its adjacent regions in November–December 2015 were generally the same as usual. A question has arisen as to what factor led to such extreme severe haze pollution in Beijing, particularly during these two months, and what the quantitative relationship was between the haze pollution and atmosphere dynamics. To follow up, there was a question about the predictability of the anomalous severe haze pollution on hourly and daily time-scales. To date, a few studies have been performed to explore these issues, but the answers to these questions remain uncertain. Thus, the primary objectives of this paper can be summarized in two ways. The first is to examine the possible causes of the severe haze pollution in downtown Beijing in November–December 2015 on monthly to seasonal time-scales; the second is to discuss the predictability of the severe haze pollution for different lead times using a high-resolution WRF-Chem model and Global Forecast System (GFS) data.

This paper is organized as follows. The data and methods used in the diagnostic analysis and model setting in the simulation were described in Section 2. The major results of the diagnostic analysis and simulations are presented in Section 3. Some uncertainty or unresolved phenomena are discussed in Section 4. The primary conclusions are summarized in Section 5.

2. Data, model and methodologies

2.1. Data and research area

During this study, the hourly $PM_{2.5}$ (particle matter with aerodynamic diameter <2.5 μm) concentration in downtown Beijing was derived from eight stations operated by the Ministry of Environmental Protection of the People's Republic of China over the period of November–December 2015 (Fig. 1). Moreover, the $PM_{2.5}$ concentration data derived from the American Embassy station were also used for comparing and filling in the missing data followed by regression analysis. From November 1st to December 31st 2015, the missing rates of hourly $PM_{2.5}$ concentration records at the American Embassy station and the average from the eight operational stations were 0.68% (10 h missing) and 3.62% (53 h missing), respectively. In fact, the hourly $PM_{2.5}$ records from the American Embassy station are highly consistent with the average from the eight stations. The correlation coefficient is 0.96, which is significant at the 0.01 level ($p < 0.01$ for short). The difference in their mean values is only 0.81 μg/m^3. To represent the data across the city better, we take the average records from the eight stations as the actual $PM_{2.5}$ concentration for downtown Beijing in this study. The location of Beijing in northern China and the spatial distribution of environmental and meteorological stations in downtown Beijing are shown in the left panel and right panel in Fig. 1, respectively. The left panel in Fig. 1 also represents the model domain of the WRF-Chem simulations. Throughout the paper, the meteorological day was defined as the 20:00–20:00 time span (local time) for the daily mean values calculated here.

2.2. Model and simulation design

To examine the predictability (or feasibility of prediction) for severe haze pollution in downtown Beijing, the medium-range (10 days) and high-resolution (9 km) simulation experiments were executed by using an online-coupled WRF-Chem model (Weather Research and Forecasting model coupled with Chemistry) (version 3.3) (Grell et al., 2005; Fast et al., 2006; Kumar et al., 2014; Liu et al., 2016; Wang et al., 2016). We used meteorological forecast data from the Global Forecast System (GFS) that were produced by the National Centers for Environmental Prediction (NCEP) as the meteorological lateral boundary conditions in the simulations. Specifically, the temporary and spatial resolutions of the GFS forecast data used here are 6 h and a 1.0° × 1.0° interval, respectively. The maximum lead time (the time span of the prediction) is 240 h (10 days) for each run (or experiment), and there are 72 runs in total (from October 21st to December 31st 2015, there were 72 days in total). For example, the first run is from 20:00 PM universal time on October 21st to 20:00 PM on October 31st, the second run is from 20:00 PM on October 22nd to 20:00 PM on November 1st, and so on. Technologically, a cycle simulation scheme had been designed to perform the runs. The primary settings and schemes used in the WRF-Chem simulations are shown in Table 1. The schemes used in our simulations are generally similar to those in Crippa et al. (2016), except for a few differences. To better capture the process of haze occurrence near the surface, there are 13 levels designed for use at under 1500 m. A high spatial resolution (0.1° × 0.1°) of anthropogenic emissions (monthly in 2012) was used in the simulation, which was provided by the MEIC group (Multi-resolution Emission Inventory for China) (Zhang et al., 2009; Li et al., 2015).

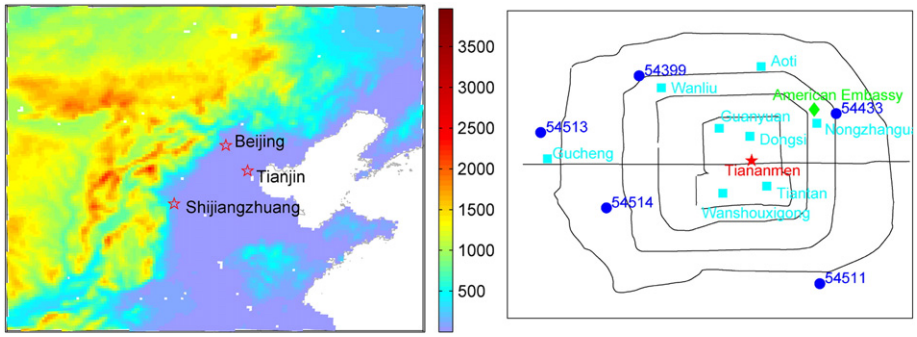

Fig. 1. Topographic map of northern China (left panel) and the environmental monitoring sites operated by the Ministry of Environmental Protection of the People's Republic of China (cyan square) and American Embassy (green diamond) and meteorological stations derived from China Meteorological Administration (blue dot) in downtown Beijing (right panel).

2.3. Mathematical methods

Common statistical methods such as comparative analysis (e.g., anomalies in a special year compared to the climatology) and Pearson correlation analyses with a two-tailed Student's *t*-test are applied in this research. To evaluate the performance of the WRF-Chem model combined with GFS simulations, statistics such as the correlation coefficient (r), root mean square error (RMSE) and normalized mean error (NME) were used. The NME value is defined as follows:

$$\mathrm{NME} = \frac{\sum_{i=1}^{N} |C_m - C_o|}{\sum_{i=1}^{N} C_o} \quad (1)$$

where C_m is the model-estimated concentration at station i, C_o is the observed concentration at station i, and N equals the number of estimate-observation pairs drawn from all the valid monitoring station data for the comparison time period of interest (Boylan and Russell, 2006). Generally, a high positive r suggests that the fluctuations in the model-estimated $PM_{2.5}$ concentration are consistent with the observed ones; the lower RMSE and NME suggest that the bias between the estimated and observed data are smaller, and vice versa. A Reduction of Error (RE) was also used to evaluate the skill of the prediction. Previous studies suggested that the RE is an extremely rigorous verification statistic because it has no lower bound, with RE > 0 indicating a skillful estimation, RE > 0.2 indicating a reliable estimation and RE = 1.0 indicating a perfect estimation (Gong and Luterbacher, 2008; Zhang et al., 2016). RE can be calculated by using the following equation:

$$\mathrm{RE} = 1.0 - \left[\frac{\sum_{i=1}^{N} (C_o - C_m)^2}{\sum_{i=1}^{N} \left(C_o - \overline{C}_o\right)^2}\right] \quad (2)$$

where C_m, C_o and N are the same as above, and $\overline{C}_o$ is the mean of the dependent data set (namely, the observed data) used for calibration (Fritts, 1976).

Table 1
List of the main settings or schemes used in the WRF-Chem simulations.

Simulation settings	Values
Domain size	133 × 124 cells (>1.3 million km^2)
Horizontal resolution	9 km
Vertical resolution	30 levels up to 50 hPa
Time step for physics	45 s
Time step for chemistry	3 min
Physics option	**Adopted scheme**
Microphysics	WRF Single-Moment 6-class scheme
Longwave radiation	Rapid radiative transfer model (RRTM)
Shortwave radiation	Goddard
Surface layer	Monin–Obhukov similarity
Land surface	Noah Land Surface Model
Planetary boundary layer	Yonsei University scheme (YSU)
Cumulus parameterizations	Grell 3D
Chemistry option	**Adopted scheme**
Photolysis	Fast-J photolysis
Gas phase chemistry	CBM-Z
Aerosols	MOSAIC with 4 sectional bins
Anthropogenic emissions	MEIC with spatial resolution of 0.1° × 0.1°
Biogenic emissions	Guenther, from USGS land use classification

3. Results

3.1. Local meteorological conditions and large-scale atmosphere circulations

The daily mean $PM_{2.5}$ concentrations in downtown Beijing over November–December 2015 are presented in Fig. 2. The standard deviations for the 24-hour records from each day are indicated by error bars. Days with a high $PM_{2.5}$ concentration and a small error bar, such as December 1st and December 25th, indicate heavy pollution throughout the day. By contrast, a large error bar generally indicates an intense fluctuation in the $PM_{2.5}$ concentration, which may be a reflection of the accumulation or elimination of pollutants, or both of them. It is clear that most (36 days, or approximately 59%) of the daily $PM_{2.5}$ concentrations were higher than 75 μg/m^3, which suggest pollution according to the ambient air quality standards of China. The mean concentration over this period was 140.6 μg/m^3, which is far larger than the annual mean from 2015 (80.6 μg/m^3 from the Beijing Municipal Environmental Protection Bureau). During the November–December 2015 period, extreme severe pollution occurred on the 1st and 25th of December, and the daily mean $PM_{2.5}$ concentrations in downtown Beijing exceeded 500 μg/m^3, which was very unusual. Generally, the high $PM_{2.5}$ concentration records suggested that severe or even extreme haze pollution occurred in Beijing in November–December of 2015.

Many studies have demonstrated that the variability in haze pollution (as indicated by the $PM_{2.5}$ concentration and/or visibility) on a synoptic time-scale were closely related to the local meteorological conditions, such as the wind speed, wind direction, relative humidity, boundary layer height (Guo et al., 2014; Wu et al., 2014; Zhang et al., 2015b; Zhang et al., 2015c). The mean relative humidity and wind speed in November–December from 1981 to 2010 (Clim) and 2015 as evaluated from the records taken at the five synoptic meteorological stations located in downtown Beijing (shown in Fig. 1) are presented in Fig. 3a and Fig. 3b, respectively. As expected, the mean relative humidity (wind speed) in downtown Beijing over November–December

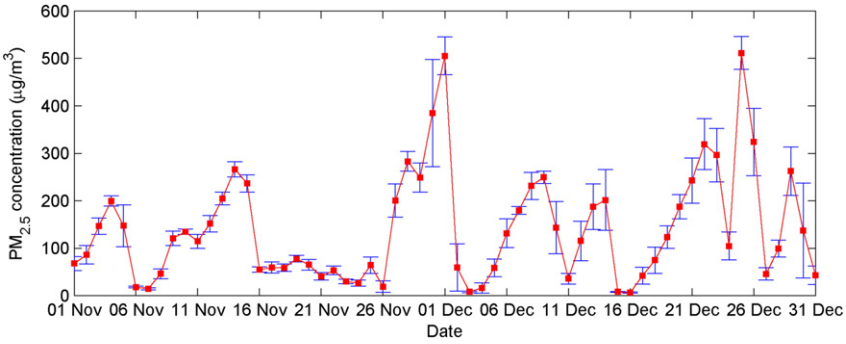

Fig. 2. The daily mean $PM_{2.5}$ concentration in downtown Beijing over November–December 2015 (the error bars denote the standard deviation in 24-hour records).

2015 was distinctly higher (lower) than the climatological means. The mean relative humidity in November–December 2015 (72.4%) increased by 38.2% compared to the climatological mean (52.4%). By contrast, the mean wind speed over November–December 2015 (1.49 m/s) was reduced by 24.1% compared to the climatological mean (1.96 m/s). Based on the EAR-Interim reanalysis data, the boundary layer height in downtown Beijing was also examined (Fig. 3c), and in November–December 2015 (385.3 m), it was reduced by 14.2% compared to the climatological mean (449.3 m). Since the boundary layer height is closely related to the inversion condition, the mean temperature profiles in the lower-middle troposphere were analyzed (Fig. 3d). In downtown Beijing, the air temperature during November–December 2015 was cooler than usual in the lower troposphere (at approximately 850 hPa), but it was warmer than usual from the middle to upper troposphere. This result suggested that the air in the lower troposphere over this area was more stable, which further denoted a strengthened atmospheric inversion and a reduced boundary layer height in November–December 2015.

The local meteorological conditions in downtown Beijing during the November–December 2015 period can be summarized to show: the weakened winds (calm winds), lower boundary layer, strengthened temperature inversion, and higher relative humidity, which are all favorable for the accumulation and hygroscopic growth of pollutants. They are very conducive to the formation of haze pollution in the context of pollutant emission. Thus, the anomalously severe haze pollution in November–December 2015 could be directly attributed to the unusual local weather conditions, at least partially. We wonder what caused the anomalous changes in the local weather conditions, and what the links are between the anomalous local weather conditions and the larger-scale atmosphere circulations.

To examine the relation between the local weather conditions and large-scale atmospheric circulation, we conducted further analysis. Most of the previous studies have suggested that the winter (December to February) haze pollution in the Beijing-Tianjin-Hebei region was closely related to the variation in atmosphere circulations in the mid-high latitudes (Zhang et al., 2016), or even the extent of Arctic sea ice (Wang and Chen, 2016). First, we examined the climatological mean (refer to 1981–2010) fields of sea level pressure (SLP), low-level wind at 850 hPa (U&V850), geopotential height at 500 hPa (H500) and zonal wind at 200 hPa (U200) as averaged over November–December based on ERA-Interim reanalysis data (Fig. 4) (Dee et al., 2011). In the climatological mean fields over November–December, Beijing is located in the eastern edge of Siberia-Mongolia high at sea level pressure (Fig. 4a) and the western edge of East Asian trough at the middle troposphere (Fig. 4c) and the entrance of East Asian jet stream at the upper troposphere (Fig. 4d), which are accompanied by the northwesterly wind at the lower troposphere (Fig. 4b). Theoretically, the configuration of these atmospheric conditions is not conducive to the accumulation of pollutants and then the formation of haze pollution.

To investigate the changes in these meteorological fields that occurred in November–December 2015, we examined the anomaly fields of SLP, U&V850, H500 and U200 (Fig. 5). The spatial distribution of the SLP anomaly shows that the main part of the Siberia-Mongolia high was weaker than normal in November–December 2015 (Fig. 5a).

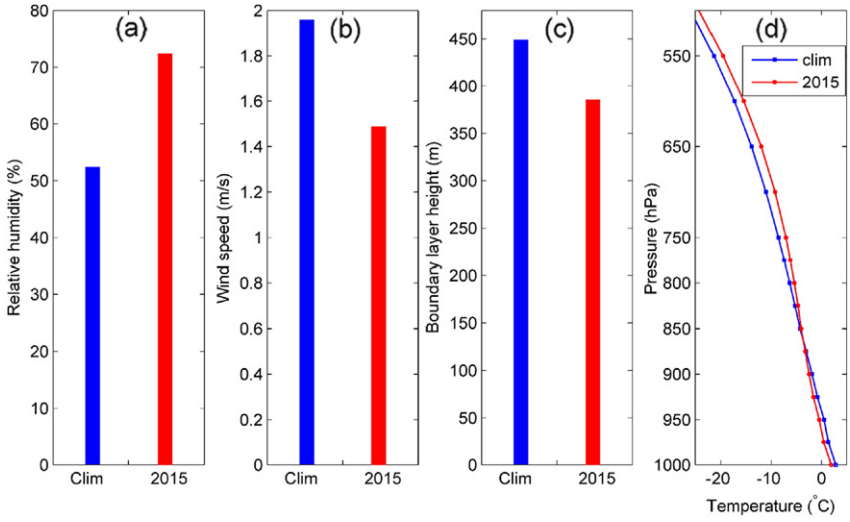

Fig. 3. The climatological mean (blue bar/line) relative humidity (a), wind speed (b), boundary layer height (c) and temperature profile (d) in downtown Beijing compared to those in 2015 (red bar/line).

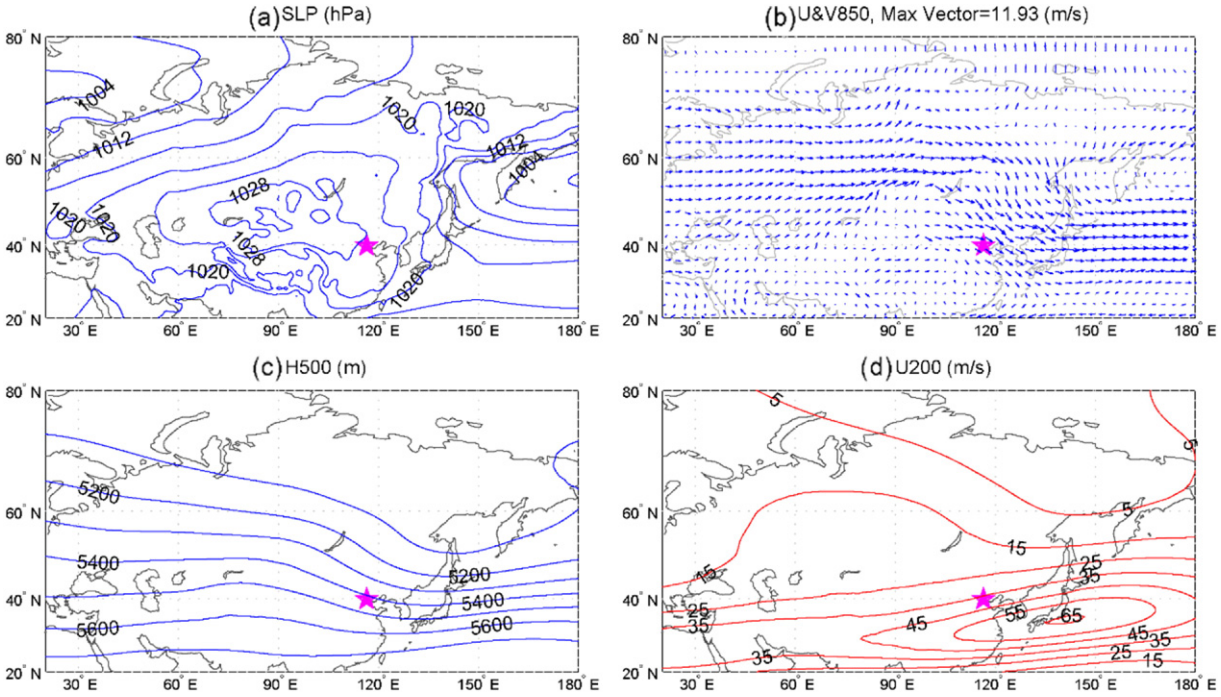

Fig. 4. The climatological mean fields of SLP (a), low-level wind at 850 hPa (b), geopotential height at 500 hPa (c) and zonal wind at 200 hPa (d) as averaged for November–December from 1981 to 2010 based on ERA-Interim reanalysis (red star indicates the location of Beijing).

However, the pressure was strengthened in the regions from the eastern edge of Siberia-Mongolia high through the East China Sea to the northwest Pacific Ocean. The pressure increase for the ocean and the decrease on the continent reflect a weakened East Asian winter monsoon, presumably due to the reduced land-sea thermal contrast in the lower troposphere. Furthermore, the East Asian jet stream in the upper troposphere (Fig. 5d) and the East Asian trough in the middle troposphere (Fig. 5c) became weaker, which are not favorable conditions for inducing the cold polar air southward. Correspondingly, the anomalous southeasterly winds dominated Beijing during November–December 2015 instead of the northwesterly wind in the climatological mean wind field (Fig. 5b), which was unfavorable (favorable) to the dissipation of pollutants (formation of haze pollution) due to a reduced capacity for air clearness.

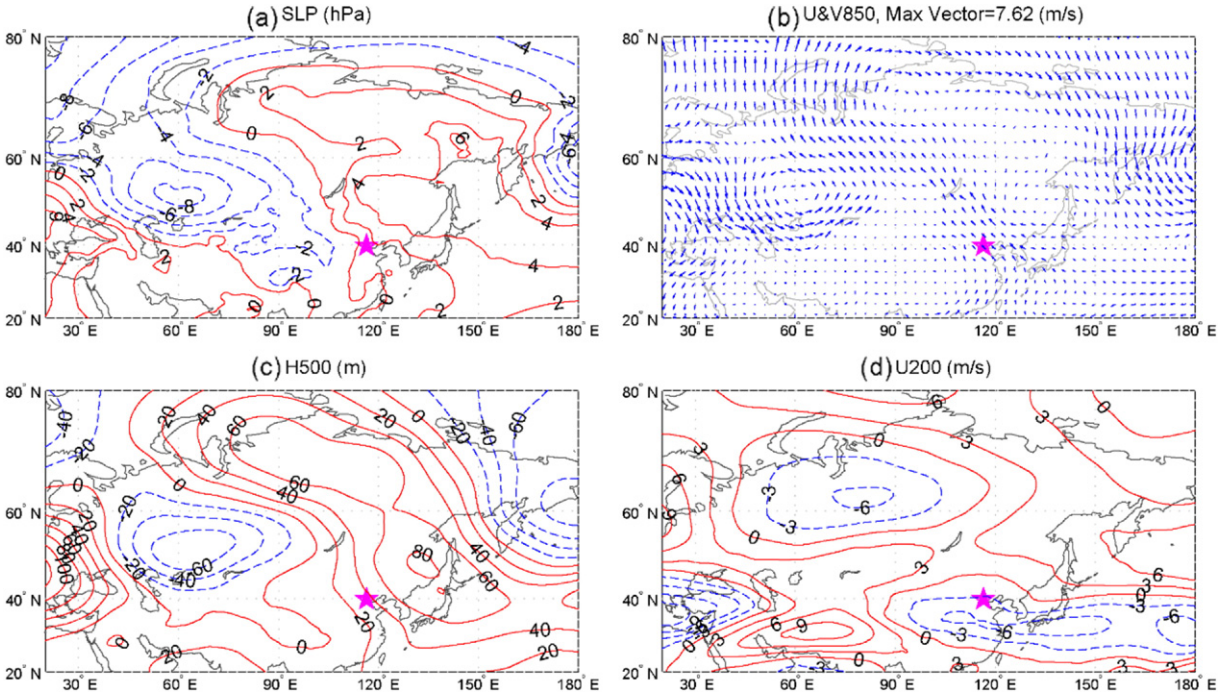

Fig. 5. The anomaly fields of SLP (a), low-level wind at 850 hPa (b), geopotential height at 500 hPa (c) and zonal wind at 200 hPa (d) in November–December 2015 based on ERA-Interim reanalysis (red star indicates the location of Beijing).

High humidity conditions are known to promote the hygroscopic growth of particles, which subsequently cause a high mass concentration of pollutants and then severe haze episodes in Beijing or eastern China (Wang et al., 2012; Guo et al., 2014; Zhang et al., 2015b). The meteorological station records as described above also demonstrated that the relative humidity in downtown Beijing over November–December 2015 increased by 38.2%. However, we wondered in which conditions the high humidity could be maintained for two months in the local region. Generally, persistently high humidity is associated with large-scale anomalous water vapor transport. To elucidate this issue, we examined the vertically integrated water vapor as derived from ERA-Interim reanalysis data. It is quite clear that the water vapor over most of northern China in November–December 2015 was higher than the climatology (Fig. 6a). This finding confirms that the anomalously higher water vapor in such a large region could help maintain the higher humidity conditions in downtown Beijing.

To evaluate the clearance capacity of the atmosphere, we further examined the kinetic energy (Fig. 6b). The greater kinetic energy of the atmosphere could have a greater capacity to clean the air by removing or transporting the pollutants, and vice versa. This capacity warrants that the kinetic energy should be a comprehensive index to indicate haze pollution in Beijing. As expected, compared to the climatological means, the vertical integral of kinetic energy (which was derived from the ERA-Interim reanalysis directly) decreased in November–December 2015 over most of northern China, especially around Beijing and its adjacent areas (Fig. 6b). The decreased kinetic energy indicates that the atmosphere was more stable or sluggish in November–December 2015 than usual, and the clearance capacity of the atmosphere decreased inevitably, which were all favorable to the accumulation of air pollutants and the formation of haze pollution.

It should be noted that most of the emission discharges and haze pollution primarily occurred within the planetary boundary layer. That is, it is necessary to understand the distribution of kinetic energy at different levels and the possible links between the air activity in the near surface and middle-upper troposphere or even the stratosphere. We examined the zonal, meridional, and vertical winds from the surface to the lower stratosphere (Fig. 7). Compared to the climatological mean (Fig. 7a), the zonal winds clearly decreased from the lower troposphere to the lower stratosphere over most of the section in November–December 2015 (Fig. 7b). The negative center is located at the tropopause area from approximately 30°N to 36°N, which suggested that the East Asian jet entrance (especially in the center-north) is significantly weaker than usual. Corresponding to the reduced zonal winds, the anomalous sinking motion and southerly winds occurred from the tropopause to the surface, which reflected that the northerly winds decreased in November–December 2015. Generally, the kinetic energy (or simply the wind speed) transfer from the free atmosphere to the planetary boundary layer can cause an energy increase in the near surface, which are beneficial conditions for the spread or diffusion of pollutants. In November–December 2015, the large decrease of kinetic energy in the middle-upper troposphere would lead to little energy transfer to the planetary boundary layer, so the air tended to be more stagnant and then haze pollution occurred easily. Thus, the abnormal changes in the upper troposphere may be the trigger points for the anomalies in the middle-lower troposphere and local conditions.

3.2. Evaluation of the medium-range forecast tests of $PM_{2.5}$ concentrations

Based on the WRF-Chem model and GFS forecast data, a series of high-resolution simulation experiments for the medium-range $PM_{2.5}$ concentration forecast in downtown Beijing during November–December 2015 has been performed. As mentioned above, the maximum lead time for the prediction is 10 days for each run, which consisted of day 1 (1–24 h), day 2 (25–48 h), day 3 (49–72 h), …, day 10 (217–240 h). We compared the features of the spatial distribution of simulated $PM_{2.5}$ concentrations at different lead times to the observed during the research period. The observed mean $PM_{2.5}$ concentrations over most of northern China during November–December 2015 is shown in Fig. 8a. Most of Beijing, Tianjin, the middle-southern area of Hebei province and the northwest part of Shandong province experienced moderate ($\geq$115 μg/m^3) to high levels ($\geq$150 μg/m^3) of pollution during the two months. The simulated mean $PM_{2.5}$ concentrations for prediction 1 day (day 1), 4 days (day 4) and 7 days (day 7) in advance are shown in Fig. 8b, c and d, respectively. Intuitively, the spatial distribution patterns of the simulated mean $PM_{2.5}$ concentrations at different lead times are generally consistent with one another. Heavy pollution occurred from the middle-southern region of Hebei province along the foot of Taihang Mountain to the Beijing areas. To understand the similarity between the model-estimated and observed spatial patterns in $PM_{2.5}$ concentrations in quantitative terms, the correlation coefficients

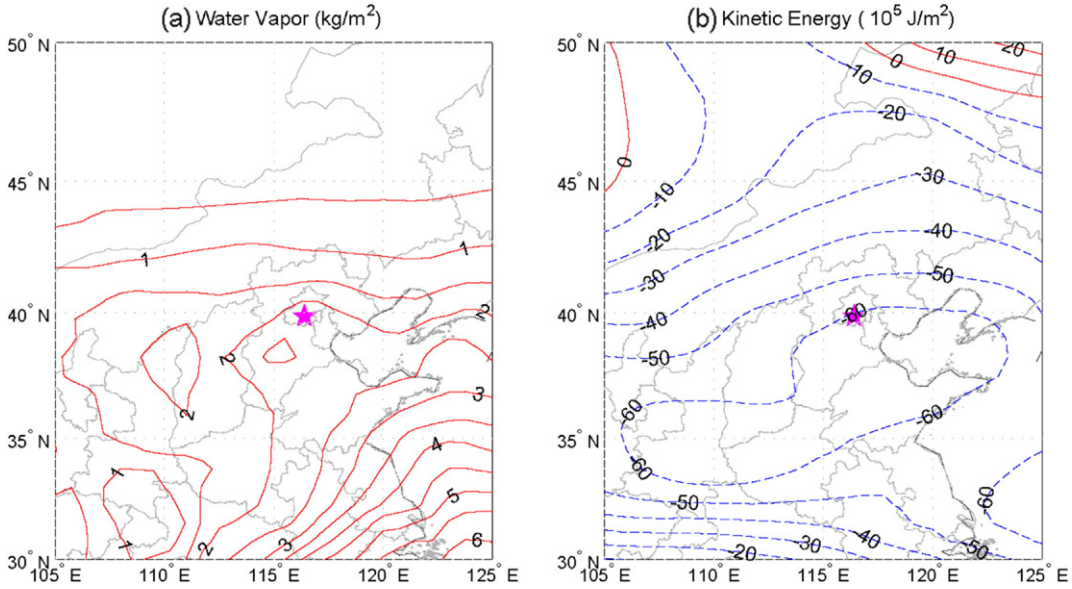

Fig. 6. The anomaly fields for the vertical integral of water vapor (a) and kinetic energy (b) in November–December 2015 based on ERA-Interim reanalysis (red star indicates the location of Beijing).

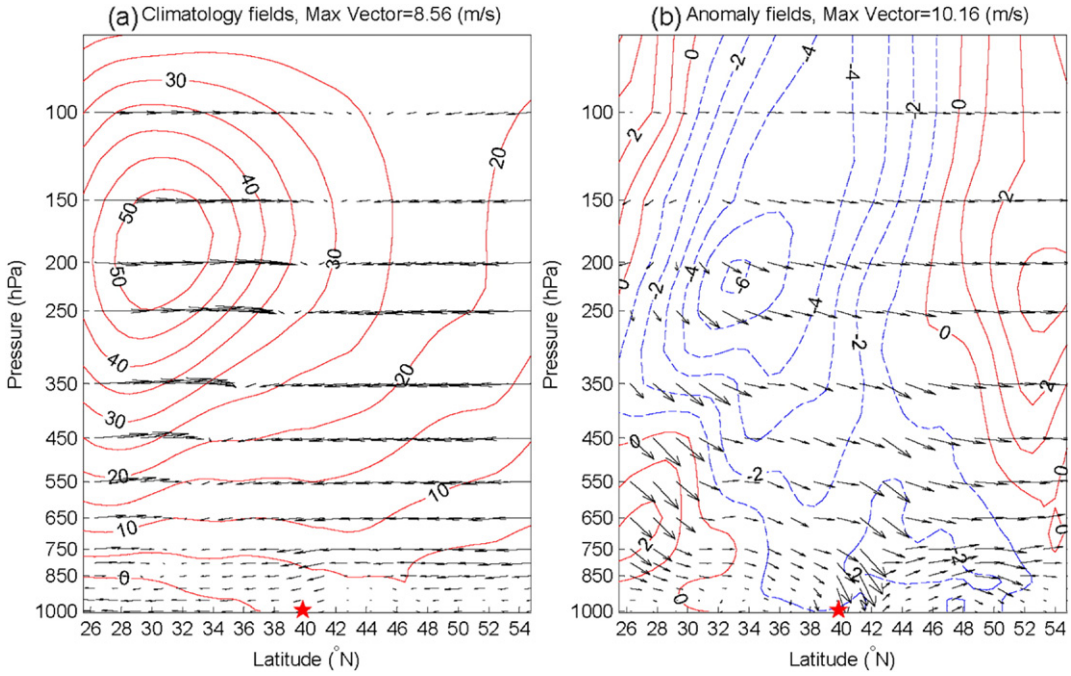

Fig. 7. The climatology (a) and anomaly (b) zonal, meridional and vertical winds along 114–118°E (the meridional and vertical winds are shown as vectors and zonal winds as contours, all of them are in unit of m/s. To facilitate comparison, the vertical winds have been multiplied by 100).

between the observed mean $PM_{2.5}$ concentrations at all stations located in the simulation domain and the corresponding $PM_{2.5}$ concentrations derived from the simulation at different lead times were calculated (Table 2). From day 1 to day 10, the spatial pattern correlation coefficients are larger than 0.73 ($p < 0.01$). The high correlation coefficients suggested that all the simulations at different lead times can reasonably predict the spatial distribution patterns of the $PM_{2.5}$ concentrations. In other words, the model-estimated $PM_{2.5}$ concentrations over a spatial distribution would be highly reliable at a medium-range time-scale.

The primary objective of the simulation is to investigate the predictability of the $PM_{2.5}$ concentration (haze pollution) in downtown Beijing on daily and hourly time-scales. To examine the predictability of the model, the temporal series of $PM_{2.5}$ concentrations that were confined to downtown Beijing were extracted from the model outputs. The

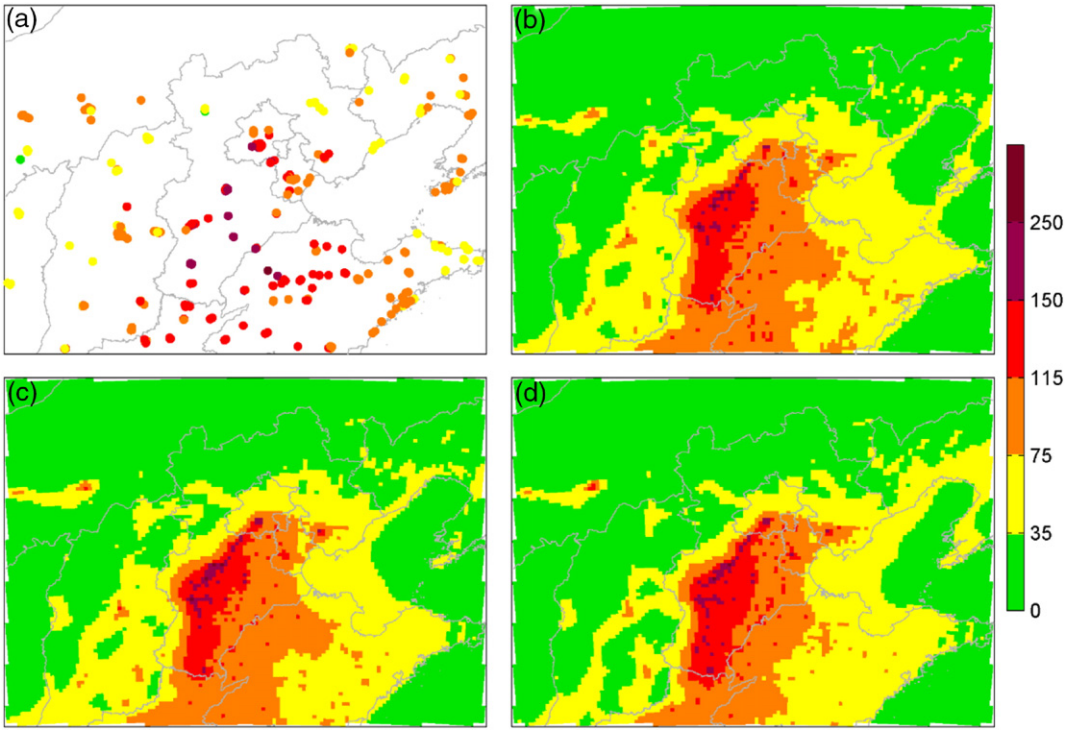

Fig. 8. The observed mean $PM_{2.5}$ concentration (a) and the simulated mean $PM_{2.5}$ concentration for prediction day 1 (b), day 4 (c) and day 7 (d).

Table 2
Correlation coefficients between the observed and simulated spatial distribution patterns of $PM_{2.5}$ concentrations.

	Day 1	Day 2	Day 3	Day 4	Day 5	Day 6	Day 7	Day 8	Day 9	Day 10
r	0.751	0.762	0.756	0.760	0.767	0.737	0.745	0.771	0.765	0.758

(All the correlation coefficients are significant at the 0.01 confidence level).

observed daily $PM_{2.5}$ concentrations and the simulated daily $PM_{2.5}$ concentrations at different lead times are plotted in Fig. 9. Intuitively, the day-to-day variation trends in the model-estimated daily $PM_{2.5}$ concentrations at different lead times are largely consistent with the observed ones, such as the slow increase in $PM_{2.5}$ concentrations from November 6th to 14th, November 26th to 28th, December 3rd to 9th, and December 16th to 21st; and for the relatively quick decrease in $PM_{2.5}$ concentrations during the periods of November 15th to 24th, December 9th to 11st, December 15th to 16th, December 23rd to 24th and 29th to 31st. However, there are two episodes with large biases that occurred from November 30th to December 1st and December 25th to 26th, which were the most seriously polluted periods during the two months. However, the daily mean $PM_{2.5}$ concentrations are underestimated in most of the simulations. The model-estimated daily mean $PM_{2.5}$ concentrations varied from 113.9 μg/m^3 to 135.6 μg/m^3 with an average of 124.2 μg/m^3. That is, the model-estimated daily mean $PM_{2.5}$ concentrations at different lead times were approximately 3.6% to 19.0% lower than the observed concentrations.

To quantitatively understand the capacity of the WRF-Chem model combined with the GFS simulations in predicting the haze pollution in downtown Beijing at different lead times, the statistics including the *r*, RE, RMSE and NME were calculated on daily and hourly time-scales, respectively (Fig. 10). Generally, the statistics on an hourly time-scale are consistent with those on a daily time-scale. The correlation coefficients decreased when the lead time was prolonged on both time-scales. On a daily (hourly) time-scale, the correlation coefficients varied from 0.17 (0.13) to 0.64 (0.58) with an average of approximately 0.44 (0.39). According to the critical values for the Pearson correlation, all the correlation coefficients on both the daily and hourly time-scales are significant at the 0.01 confidence level, with exceptions for day 9 and day 10. Similar to the correlation coefficients, the RE values also decreased when the lead time was prolonged on both time-scales. On a daily (hourly) time-scale, the RE varies from −0.26 (−0.34) to 0.47 (0.39) with an average of approximately 0.15 (0.07). On a daily time-scale, the RE values are larger than 0.0 and 0.2 in predictions of 1 to 8 days in advance and in predictions of 1 to 5 days in advance, respectively. On an hourly time-scale, the RE values are also larger than 0.2 in predictions of 1 to 5 days in advance.

In contrast to the RE and *r*, the RMSE and NME values increased gradually when the lead time was prolonged on both time-scales. On a daily (hourly) time-scale, the RMSE increased from 85.8 (103.1) to 130.0 (150.7) with an average of approximately 106.7 (125.1); the NME increased from 37.5 (44.6) to 63.7 (73.3) with an average of approximately 49.3 (57.7). According to the statistics, it can be concluded that by using the WRF-Chem model and GFS data, the predictions of daily and hourly mean $PM_{2.5}$ concentrations in downtown Beijing for November–December 2015 are generally reliable for the maximum lead times of 8 days and 5 days, respectively. In other words, the maximum lead time for predicting the daily mean $PM_{2.5}$ concentration is overall larger than the prediction for the hourly mean $PM_{2.5}$ concentration, and the predictability of the daily mean $PM_{2.5}$ concentration is overall better than that of the hourly concentration.

As demonstrated above, the severe haze pollution in November–December 2015 could be attributed to the anomalous local weather conditions, in addition to the pollutant emission, such as the reduced wind speed and the increased relative humidity. We further examined what the prediction efficiency of the simulations for the local wind speed and relative humidity were at different lead times. The observed daily mean relative humidity and wind speed in downtown Beijing for November–December 2015 in comparison to the model-estimated concentration within predictions of 1 to 10 days in advance are presented in Fig. 11a and b, respectively. It can be observed that the daily fluctuation trends in the model-estimated local wind speed and relative humidity are generally consistent with the station-observed findings with a few exceptions. To measure the consistency quantitatively, we estimated the *r* and RE statistics for the relative humidity and wind (Fig. 12). On a daily (hourly) time-scale, the *r* between the simulated relative humidity and the observed humidity varies from 0.43 (0.39) to 0.69 (0.67) with an average of approximately 0.57 (0.54), and all of them are significant at a 0.01 confidence level (Fig. 12a); the *r* between the simulated wind speed and the observed one varies from 0.27 (0.23) to 0.91 (0.80) with an average of approximately 0.73 (0.58); all of them are also significant at the 0.01 confidence level with one exception in day 10 (Fig. 12b). As expected, the *r* decreased gradually with a prolonged forecasting time. Unlike the correlation coefficients, the RE values for the relative humidity and wind speed simulations decreases dramatically compared to the $PM_{2.5}$ simulations. On a daily (hourly) time-scale, the RE for the relative humidity at different lead times varies from −0.61 (−0.40) to 0.02 (0.14) with an average of approximately −0.24 (−0.08); and it varies from −6.14 (−4.91) to −3.37 (−3.16) with an average of approximately −4.32 (−3.78) for wind speeds.

Why did the RE values drop dramatically while the correlation coefficients were reasonably high for the humidity and wind speed simulations? We speculated that these phenomena could be primarily attributed to the large deviations between the simulations and the observations, although their fluctuations were consistent. Intuitively, the simulations systematically overestimated the wind speed and underestimated the relative humidity simultaneously. As shown in Fig. 3, the mean relative humidity and wind speed in downtown Beijing over November–December 2015 were 72.4% and 1.49 m/s, respectively. For the predictions from 1 to 10 days in advance, the model-estimated

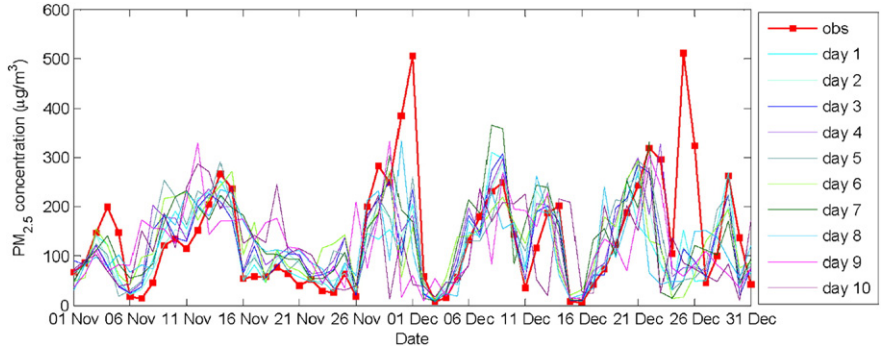

Fig. 9. Curves of the observed daily mean $PM_{2.5}$ concentrations and the simulated daily mean $PM_{2.5}$ concentrations in different leading times (day1 to day10).

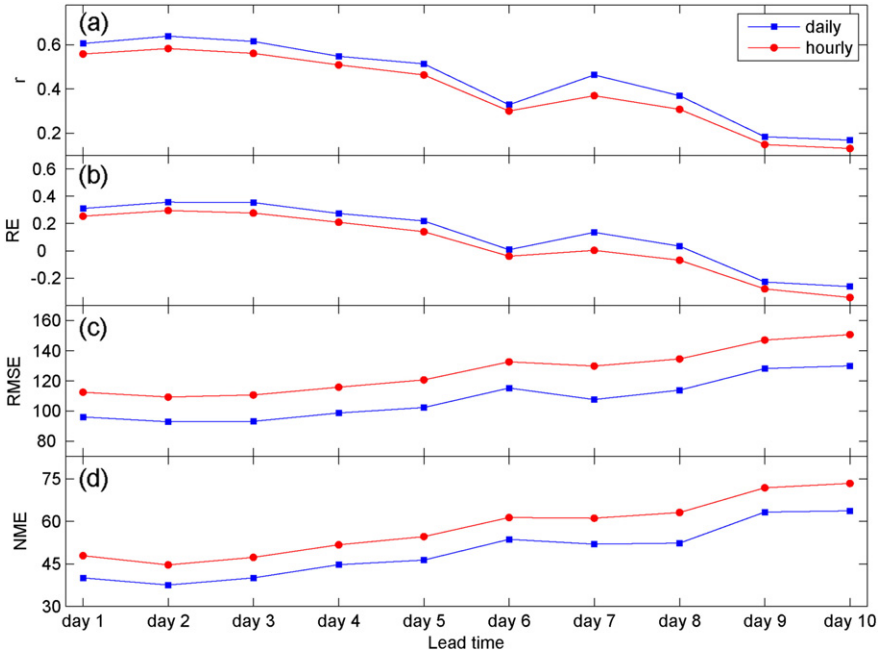

Fig. 10. Statistics for the observed mean $PM_{2.5}$ and simulated concentrations for different lead times on daily and hourly time-scales (the critical values for *r* that are significant at the 0.01 confidence level on daily and hourly time-scales are 0.33 and 0.18, respectively).

mean relative humidity varied from 59.9% to 65.6% with an average of 63.2%; the model-estimated mean wind speed varied from 2.40 m/s to 2.84 m/s with an average of 2.63 m/s. The model-estimated wind speeds at different lead times were approximately 60.8% to 90.4% with the average of 76.3% being higher than the observed wind speed; the model-estimated relative humidities were approximately 9.4% to 17.3% with an average of 12.8% lower than the observed relative humidity. In view of these findings, the high correlations accompanied by the low RE statistics between the observed and the simulated humidity and wind speed are reasonable overall. The overestimated wind speed and/or the underestimated humidity are conducive to underestimating the $PM_{2.5}$ concentration in simulations due to their important roles in the formation, accumulation, or diffusion of air pollutants. For example, during episodes of extremely serious haze pollution (as indicated by the shaded bars in Fig. 11), the relative humidities (wind speeds) were distinctly underestimated (overestimated), especially around the 25th of December. Thus, the simulations almost failed to predict the extremely severe haze pollution from the two episodes due to their poor performance in capturing the wind speed and relative humidity.

4. Discussions

In this study, the kinetic energy index was used in an innovative manner to evaluate the clearance capacity of the atmosphere for air

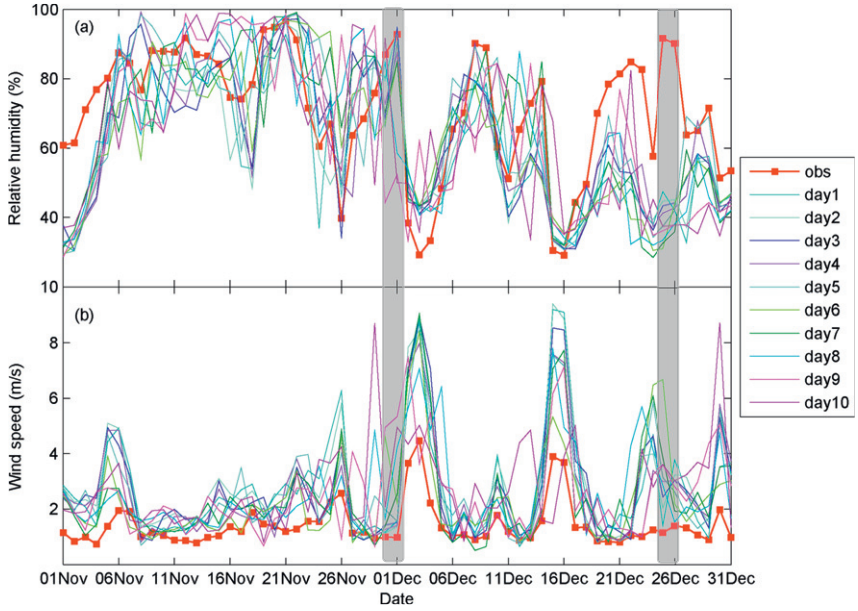

Fig. 11. Curves of the observed daily mean relative humidity (a) and wind speed (b) compared to the simulated at different lead times (the two shaded bars indicate the extremely haze pollution days).

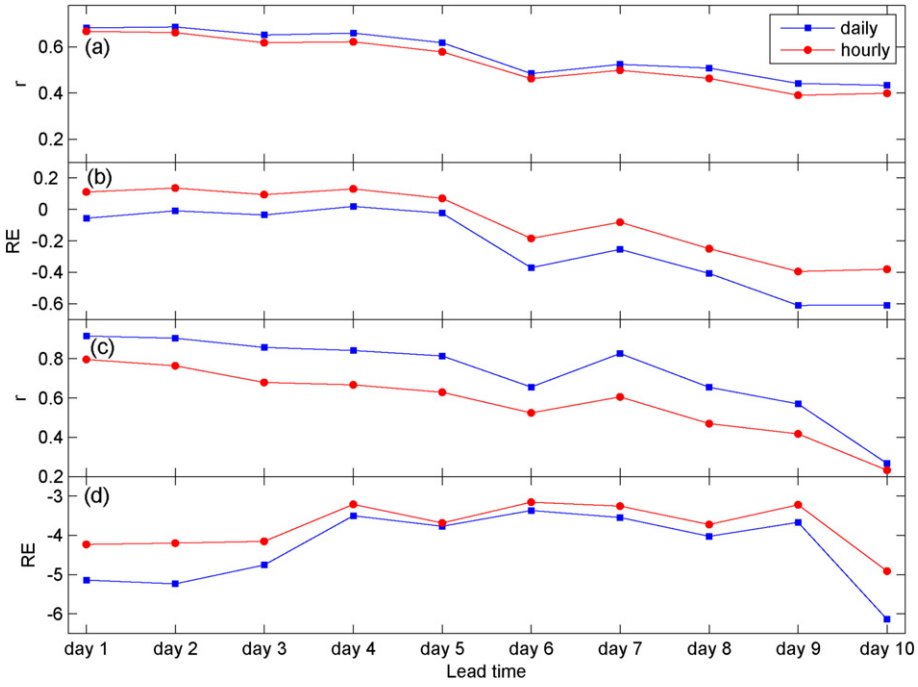

Fig. 12. Statistics for the observed relative humidity (a, b) and wind speed (c, d) and the simulated at different lead times on daily and hourly time-scales (the critical values for *r* significant at the 0.01 confidence level on daily and hourly time-scales are 0.33 and 0.18, respectively).

pollutants in downtown Beijing on monthly to seasonal time-scales. Generally, the kinetic energy transfer from the free atmosphere to the planetary boundary layer can cause an energy increase at the near-surface, which is favorable for the transport, diffusion, and removal of pollutants. Compared to the climatologically normal level, the kinetic energy decreased significantly in the upper troposphere and then led to a little energy transfer to the planetary boundary layer over most of northern China in November–December 2015, setting up a favorable condition for the air to be more stagnant and then leading to extreme haze pollution. Although we need more tests to make improvement (i.e., not the vertical integral for the entire air column) and evaluations, we checked that the kinetic energy index would be a great potential factor for predicting or evaluating the haze pollutions in downtown Beijing and its neighboring areas in operations in this study.

The daily variation trends in the model-estimated $PM_{2.5}$ concentrations for different lead times were highly consistent with the observed concentrations. The statistical indices suggested that a highly skillful and reliable prediction technique for the daily and hourly $PM_{2.5}$ concentration (or haze pollution) forecasts in Beijing or even in a larger region would be expected for predictions of 8 days or longer time in advance, although the predictability gradually decreased with the lead time. However, the simulations almost failed to capture the extremely severe haze pollution of the two episodes (on the 1st and 25th of December, the daily mean $PM_{2.5}$ concentrations were higher than 500 μg/m^3), which may be due to the high underestimation (overestimation) for the relative humidity (wind speed) in the simulations. However, their contributions were not identified clearly due to many uncertainties, such as the lack of absolutely real emissions on hourly and daily time-scales, and the unclear understanding of the secondary aerosols generated by the complicated physical and chemical reactions. The regional transport of pollutants played an important role in the heavy pollution in Beijing (Zheng et al., 2015a; Wang et al., 2013; Tao et al., 2014), even under stationary condition (Wang et al., 2014b).By contrast, Guo et al. (2014) noted that the impact of the regional $PM_{2.5}$ transport is negligible during the polluted period. As mentioned above, it was calm and steady overall in downtown Beijing in November–December 2015. In this study, we did not explore whether the persistently severe haze pollution was affected or not by the regional $PM_{2.5}$ transport and what the influencing processes were. To better improve the predictability and prediction precision for severe haze pollution on a medium-range time-scale, a series of emission reduction simulation tests will be necessary in the near future.

We noted that, not only on hourly time-scale but also on daily time-scale, the *r* and RE (RMSE and NME) values were abnormally low (high) for a lead time of 6 days (Fig. 10, Fig. 12). It is immediately unclear why the prediction skills for a lead time of 6 days (day 6) were relatively worse than they were for the longer lead times (i.e., day 7 and day 8). It may be an accidental phenomenon in the simulations, or it may reflect a very complicated issue that is contained in the middle-range forecast for $PM_{2.5}$ concentration.

5. Conclusions

Based on the hourly $PM_{2.5}$ concentrations and meteorological factors observed in downtown Beijing and the ERA-Interim reanalysis datasets, a series of statistical analyses have been executed to explore the possible influence of meteorological conditions on the severe haze pollution in downtown Beijing over November–December 2015. Second, a high-resolution simulation conducted by using the WRF-Chem model and GFS data were performed to examine the predictability of severe haze pollution on synoptic to medium-range time-scales. The primary conclusions can be summarized as follows.

During November–December 2015, severe haze pollution hit downtown Beijing with daily mean $PM_{2.5}$ concentrations of >140 μg/m^3. Our analysis indicates that the severe haze pollution was attributed to anomalous local meteorological conditions to a great extent, such as the decreased wind speed and boundary layer height, the increased relative humidity and thermal inversion in the lower troposphere, which are conducive to the accumulation and hygroscopic growth of pollutants and then the formation of haze pollution. We further found that the anomalous local weather conditions were closely linked to large-scale atmospheric circulations, such as the anomalous southeastern winds that were associated with the weakened land-sea thermal contrast in the lower troposphere, the weakening of the East Asian trough

in the middle troposphere and East Asian jet stream in the upper troposphere, and the anomalously higher water vapor over most of northern China. A preliminary inference showed that the abnormal changes at the tropopause may be a trigger point for the anomalous middle-lower troposphere and local meteorological conditions. The kinetic energy index was used, and the results showed that this index would be a great indicator for evaluating or predicting the haze pollution in Beijing and its adjacent areas on monthly to seasonal time-scales.

The simulations showed that the WRF-Chem model combined with GFS data can capture the spatial distribution patterns of $PM_{2.5}$ concentrations for predictions of 1 to 10 days in advance. The variation trends in the $PM_{2.5}$ concentration for downtown Beijing were generally in good predictability on both daily and hourly time-scales, although they decreased gradually as the lead times were prolonged. The predictability of the daily mean $PM_{2.5}$ concentration is slightly better than that of the hourly concentration. The statistical indices suggested that the predictions of daily and hourly mean $PM_{2.5}$ concentrations in downtown Beijing for November–December 2015 were generally skillful and reliable for maximum lead times of 8 days and 5 days, respectively. Simulations for $PM_{2.5}$ concentrations not only depend on the pollutant emission, parameter settings and model itself, but also depend more on the initial meteorological fields and lateral boundary conditions. To improve the weather forecast, a highly skillful and reliable prediction technique for the daily and hourly $PM_{2.5}$ concentration (or haze pollution) in Beijing or even over larger areas on a medium-range time-scale would be expected.

Acknowledgements

This study was supported by the Beijing Municipal Natural Science Foundation (Grant no. 8152019), National Key Technologies R & D Program of China (Grant no. 2014BAC23B03), National Natural Science Foundation of China (Grant no. 41621061), Beijing Municipal Science & Technology Commission (Grant no. Z161100004516018) and project PE17010 of the Korea Polar Research Institute (PE17010).

References

Boylan, J.W., Russell, A.G., 2006. PM and light extinction model performance metrics, goals, and criteria for three dimensional air quality models. Atmos. Environ. 40, 4946–4959.
Cao, Z.Q., Sheng, L.F., Liu, Q., Yao, X.H., Wang, W.C., 2015. Interannual increase of regional haze-fog in North China Plain in summer by intensified easterly winds and orographic forcing. Atmos. Environ. 122, 154–162.
Chan, C.K., Yao, X., 2008. Air pollution in mega cities in China. Atmos. Environ. 42, 1–42.
Cheng, X.G., Zhao, T.L., Gong, S.L., Xu, X.D., Han, Y.X., Yin, Y., et al., 2016. Implications of East Asian summer and winter monsoons for interannual aerosol variations over central-eastern China. Atmos. Environ. 129, 218–228.
Crippa, P., Sullivan, R.C., Thota, A., Pryor, S.C., 2016. Evaluating the skill of high-resolution WRF-Chem simulations in describing drivers of aerosol direct climate forcing on the regional scale. Atmos. Chem. Phys. 16, 397–416.
Dee, D.P., Uppala, S.M., Simmons, A.J., Berrisford, P., Poli, P., Kobayashi, S., et al., 2011. The ERA-interim reanalysis: configuration and performance of the data assimilation system. Q. J. R. Meteorol. Soc. 137, 553–597.
Fast, J.D., Gustafson, W.I., Easter, R.C., Zaveri, R.A., Barnard, J.C., Chapman, E.G., et al., 2006. Evolution of ozone, particulates, and aerosol direct radiative forcing in the vicinity of Houston using a fully coupled meteorology-chemistry-aerosol model. J. Geophys. Res. Atmos. 111, D21305. http://dx.doi.org/10.1029/2005JD006721.
Feng, X., Li, Q., Zhu, Y.J., Wang, J.J., Liang, H.M., Xu, R.F., 2014. Formation and dominant factors of haze pollution over Beijing and its peripheral areas in winter. Atmos. Pollut. Res. 5, 528–538.
Fritts, H.C., 1976. Tree Rings and Climate. Academic Press, London.
Fu, H.B., Chen, J.M., 2017. Formation, features and controlling strategies of severe haze-fog pollutions in China. Sci. Total Environ. 578, 121–138.
Gao, Y., Liu, X., Zhao, C., 2011. Emission controls versus meteorological conditions in determining aerosol concentrations in Beijing during the 2008 Olympic Games. Atmos. Chem. Phys. 11, 12437–12451.
Gong, D.Y., Luterbacher, J., 2008. Variability of the low-level cross-equatorial jet of the western Indian Ocean since 1660 as derived from coral proxies. Geophys. Res. Lett. 35, L01705. http://dx.doi.org/10.1029/2007GL032409.
Grell, G.A., Peckham, S.E., Schmitz, R., Mckeen, S.A., Frost, G., Skamarock, W., et al., 2005. Fully coupled "online" chemistry within the WRF model. Atmos. Environ. 39, 6957–6975.
Guo, S., Hu, M., Zamora, M.L., Peng, J.F., Shang, D.J., Zheng, J., et al., 2014. Elucidating severe urban haze formation in China. Proc. Natl. Acad. Sci. U. S. A. 111, 17373–17378.
Han, B., Zhang, R., Yang, W., Bai, Z.P., Ma, Z.Q., Zhang, W.J., et al., 2016. Heavy haze episodes in Beijing during January 2013: inorganic ion chemistry and source analysis using highly time-resolved measurements from an urban site. Sci. Total Environ. 544, 319–329.
Hang, J., Luo, Z., Wang, X., He, L., Wang, B., Zhu, W., 2017. The influence of street layouts and viaduct settings on daily CO exposure and intake fraction in idealized urban canyons. Environ. Pollut. 220, 72–86.
Hien, P.D., Loc, P.D., Dao, N.V., 2011. Air pollution episodes associated with East Asian winter monsoons. Sci. Total Environ. 409 (23), 5063–5068.
Jeong, J.I., Park, R.J., 2013. Effects of the meteorological variability on regional air quality in East Asia. Atmos. Environ. 69, 46–55.
Ji, W.J., Zhao, B., 2015. Estimating mortality derived from indoor exposure to particles of outdoor origin. PLoS One 10. http://dx.doi.org/10.1371/journal.pone.0124238.
Kumar, R., Barth, M.C., Pfister, G.G., Naja, M., Brasseur, P., 2014. WRF-Chem simulations of a typical pre-monsoon dust storm in northern India: influences on aerosol optical properties and radiation budget. Atmos. Chem. Phys. 14 (5), 2431–2446.
Li, M., Zhang, Q., Kurokawa, J., Woo, J.H., He, K.B., Lu, Z., et al., 2015. MIX: a mosaic Asian anthropogenic emission inventory for the MICS-Asia and the HTAP projects. Atmos. Chem. Phys. Discuss. 15 (23), 34813–34869.
Li, Q., Zhang, R., Wang, Y., 2016. Interannual variation of the wintertime fog–haze days across central and eastern China and its relation with East Asian winter monsoon. Int. J. Climatol. 36, 346–354.
Liu, X.Y., Zhang, Y., Zhang, Q., He, K.B., 2016. Application of online-coupled WRF/Chem-MADRID in East Asia: model evaluation and climatic effects of anthropogenic aerosols. Atmos. Environ. 124, 321–336.
Marais, E.A., Jacob, D.J., Jimenez, J.L., Campuzano-Jost, P., Day, D.A., Hu, W.W., et al., 2016. Aqueous-phase mechanism for secondary organic aerosol formation from isoprene: application to the southeast United States and co-benefit of SO_2 emission controls. Atmos. Chem. Phys. 16, 1603–1618.
Mues, A., Manders, A., Schaap, M., Kerschbaumer, A., Stern, R., Builtjes, P., et al., 2012. Impact of the extreme meteorological conditions during the summer 2003 in Europe on particulate matter concentrations. Atmos. Environ. 55, 377–391.
Quan, J.N., Liu, Q., Li, X., Gao, Y., Jia, X.C., Sheng, J.J., et al., 2015. Effect of heterogeneous aqueous reactions on the secondary formation of inorganic aerosols during haze events. Atmos. Environ. 122, 306–312.
Ramsey, N.R., Petra, M.K., Berrien, M., 2014. The impact of meteorological parameters on urban air quality. Atmos. Environ. 86, 58–67.
Streets, D.G., Fu, J.H.S., Jang, C.J., Hao, J.M., He, K.B., Tang, X.Y., et al., 2007. Air quality during the 2008 Beijing Olympic Games. Atmos. Environ. 41, 480–492.
Sun, Y.L., Wang, Z.F., Du, W., 2015. Long-term real-time measurements of aerosol particle composition in Beijing, China: seasonal variations, meteorological effects, and source analysis. Atmos. Chem. Phys. 15, 10149–10165.
Tao, M.H., Chen, L.F., Xiong, Z.X., Zhang, M.G., Ma, P.F., Tao, J.H., et al., 2014. Formation process of the widespread extreme haze pollution over northern China in January 2013: implications for regional air quality and climate. Atmos. Environ. 98, 417–425.
Tie, X., Zhang, Q., He, H., Gao, J.J., Han, S.Q., Gao, Y., et al., 2015. A budget analysis of the formation of haze in Beijing. Atmos. Environ. 100, 25–36.
Wang, H.J., Chen, H.P., 2016. Understanding the recent trend of haze pollution in eastern China: roles of climate change. Atmos. Chem. Phys. 16, 4205–4211.
Wang, T., Nie, W., Gao, J., Xue, L.K., Gao, X.M., Wang, X.F., et al., 2010. Air quality during the 2008 Beijing Olympics: secondary pollutants and regional impact. Atmos. Chem. Phys. 10, 7603–7615.
Wang, X.F., Wang, W.X., Yang, L.X., Gao, X.M., Nie, W., Yu, Y.C., et al., 2012. The secondary formation of inorganic aerosols in the droplet mode through heterogeneous aqueous reactions under haze conditions. Atmos. Environ. 63, 68–76.
Wang, Y.S., Yao, L., Liu, Z.R., Ji, D.S., Wang, L.L., Zhang, J.K., 2013. Formation of haze pollution in Beijing-Tianjin-Hebei region and their control strategies. Chin. Sci. Bull. 28, 353–363 (in Chinese).
Wang, H., Xu, J.Y., Zhang, M., Yang, Y.Q., Shen, X.J., Wang, Y.Q., et al., 2014a. A study of the meteorological causes of a prolonged and severe haze episode in January 2013 over central-eastern China. Atmos. Environ. 98, 146–157.
Wang, Z.F., Li, J., Wang, Z., Yang, W.Y., Tang, X., Ge, B.Z., et al., 2014b. Modeling study of regional severe hazes over mid-eastern China in January 2013 and its implications on pollution prevention and control. Sci. China Earth Sci. 57, 3–13.
Wang, L.T., Zhang, Y., Wang, K., Zheng, B., Zhang, Q., Wei, W., 2016. Application of weather research and forecasting model with chemistry (WRF/Chem) over northern China: sensitivity study, comparative evaluation, and policy implications. Atmos. Environ. 124, 337–350.
Whiteaker, J.R., Suess, D.T., Prather, K.A., 2002. Effects of meteorological conditions on aerosol composition and mixing state in Bakersfield, CA. Environ. Sci. Technol. 36 (11), 2345–2353.
Wu, Q.Z., Wang, Z.F., Gbaguidi, A., Gao, C., Li, L.N., Wang, W., 2011. A numerical study of contributions to air pollution in Beijing during CAREBeijing-2006. Atmos. Chem. Phys. 11, 5997–6011.
Wu, D., Liao, B.T., Wu, M., Chen, H.Z., Wang, Y.C., Liao, X.N., et al., 2014. The long-term trend of haze and fog days and the surface layer transport conditions under haze weather in North China. Acta Sci. Circumst. 34 (1), 1–11 (in Chinese).
Zhang, Q., Streets, D.G., Carmichael, G.R., He, K.B., Huo, H., Kannari, A., et al., 2009. Asian emissions in 2006 for the NASA INTEX-B mission. Atmos. Chem. Phys. 9, 5131–5153.
Zhang, X.L., Huang, Y.B., Zhu, W.Y., Rao, R.Z., 2013. Aerosol characteristics during summer haze episodes from different source regions over the coast city of North China Plain. J. Quant. Spectrosc. Radiat. 122, 180–193.
Zhang, R.H., Li, Q., Zhang, R.N., 2014. Meteorological conditions for the persistent severe fog and haze event over eastern China in January 2013. Sci. China Earth Sci. 57, 26–35.

Zhang, L., Wang, T., Lv, M.Y., Zhang, Q., 2015a. On the severe haze in Beijing during January 2013: unraveling the effects of meteorological anomalies with WRF-Chem. Atmos. Environ. 104, 11–21.

Zhang, Q., Quan, J.N., Tie, X.X., Li, X., Liu, Q., Gao, Y., et al., 2015b. Effects of meteorology and secondary particle formation on visibility during heavy haze events in Beijing, China. Sci. Total Environ. 502, 578–584.

Zhang, Z.Y., Zhang, X.L., Gong, D.Y., Quan, W.J., Zhao, X.J., Ma, Z.Q., et al., 2015c. Evolution of surface O_3 and $PM_{2.5}$ concentrations and their relationships with meteorological conditions over the last decade in Beijing. Atmos. Environ. 108, 67–75.

Zhang, Z.Y., Zhang, X.L., Gong, D.Y., Kim, S.J., Mao, R., Zhao, X.J., 2016. Possible influence of atmospheric circulations on winter hazy pollution in Beijing-Tianjin-Hebei region, northern China. Atmos. Chem. Phys. 16, 561–571.

Zheng, G.J., Duan, F.K., Su, H., 2015a. Exploring the severe winter haze in Beijing: the impact of synoptic weather, regional transport and heterogeneous reactions. Atmos. Chem. Phys. 15, 2969–2983.

Zheng, S., Pozzer, A., Cao, C.X., Lilieveld, J., 2015b. Long-term (2001−2012) concentrations of fine particulate matter ($PM_{2.5}$) and the impact on human health in Beijing, China. Atmos. Chem. Phys. 15, 5715–5725.